Available online at www.sciencedirect.com
ScienceDirect
Polymer 47 (2006) 7554–7563
polymer
www.elsevier.com/locate/polymer

Crystallization behavior of poly(L-lactic acid)

Munehisa Yasuniwa*, Shinsuke Tsubakihara, Koji Iura, Yoshinori Ono, Yusuke Dan, Kazuhisa Takahashi

Department of Applied Physics, Faculty of Science, Fukuoka University, 8-19-1 Nanakuma, Jonan-ku, Fukuoka 814-0180, Japan

Received 15 May 2006; received in revised form 22 August 2006; accepted 22 August 2006
Available online 11 September 2006

Abstract

The crystallization behavior of poly(L-lactic acid) was studied in the range of 80–160 °C. The peak crystallization time (τ_p) was defined and obtained from the crystallization isotherm measured with a differential scanning calorimeter (DSC). Isothermal crystallization temperature (T_c) dependence of log(τ_p) discretely changed at 113 °C ($=T_b$). The linear growth rate of spherulite, G, was measured with a polarizing microscope. The T_c dependence of G and the size of the spherulite also discretely changed at T_b. Crystal structures for samples isothermally crystallized at temperatures which were higher and lower than T_b were orthorhombic (α-form) and trigonal (β-form), respectively. The discrete change of the crystallization behavior was explained by the formation of different crystal.

Keywords: Poly(L-lactic acid); Crystallization; Growth rate of spherulite

1. Introduction

Poly(L-lactic acid) (PLLA; $(-CHCH_3-CO-O-)_n$) is currently investigated for a great number of commodity applications from a view point of an environmentally degradable polymer and sustainable biomass resources [1,2]. The thermal behavior, especially melting and crystallization behavior, is an important aspect for characterizing the physical properties of PLLA. Accordingly, the characterization of its melting and crystallization behavior has been performed with various experimental techniques [3].

Many researchers have studied the crystallization behavior of PLLA under an isothermal crystallization condition. Vasanthakumari and Pennings [4], and Miyata and Masuko [5], measured the radius growth rate of spherulites (G) of PLLA film samples as a function of isothermal crystallization temperature (T_c) with optical microscopy. Their T_c dependence of G showed a bell-shaped curve. Iannace and Nicolais [6] studied isothermal crystallization behavior by thermal analysis and the T_c dependence of the crystallization half-time ($t_{1/2}$), which corresponds to an overall rate of crystallization, was reported. They presented two ranges with different slopes of the T_c dependence of $10^3/t_{1/2}$ and interpreted this result as an indication from regime II to regime III transition around 115 °C. Some other researchers also studied the T_c dependence of G with optical microscopy and reported the two bell-shaped curves which are continuously connected [7–9]. There is obvious discrepancy among these results: the T_c dependence of G expressed by the single bell-shaped curve contradicts that expressed by the two bell-shaped curves and the regime transition. It is considered for the reason of this discrepancy that the number of their data points in these studies is too small to definitely determine the curve profile. Although the change of morphology of the PLLA film samples has been studied, distinct change of spherulite morphology which corresponds to the two bell-shaped curves has not been reported [4,5,7–12].

The crystal structure of PLLA has been analyzed, and three crystal modifications, α-, β-, and γ-forms, have been found depending on the formation conditions: the α-form (pseudo-orthorhombic [13,14], pseudo-hexagonal [15], or orthorhombic [16–19]), the β-form (orthorhombic [14] or trigonal [20]), and the γ-form [22]. The most common polymorph is the α-form,

* Corresponding author. Tel.: +81 92 871 6631; fax: +81 92 865 6030.
E-mail address: yasuniwa@fukuoka-u.ac.jp (M. Yasuniwa).

0032-3861/$ - see front matter © 2006 Elsevier Ltd. All rights reserved.
doi:10.1016/j.polymer.2006.08.054

which is generally formed on crystallization from the melt or from dilute solutions. The β-form is observed at a high draw ratio and a high drawing temperature. Its packing has been interpreted as a *frustrated structure* [20,22]. The γ-form has been obtained by epitaxial crystallizations on hexamethylbenzene [21]. Hoogsten et al. explained that the helical conformations of the chains in the α- and β-structures have approximately the same energy, and that the packing must therefore be the main reason for the existence of two different crystal modifications [14]. According to this explanation, there is enough possibility of the formation of β-form through the crystallization from the melt, however, β crystal structure of the melt-crystallized sample has scarcely been investigated.

The present study deals with the crystallization behavior from the melt of PLLA in the isothermal crystallization condition. Since there is a difference in the reported results with respect to the growth rate of spherulite and the crystallization half-time, the measurements of them are made in detail. Then discrete change of crystallization is presented. In addition, the mechanism of the discrete change is investigated on the basis of the structural analysis.

2. Experimental

2.1. Sample preparation

An additive free PLLA experimental resin in a pellet form was purchased from General Science Co. Molecular weight of the sample was measured with a gel permeation chromatography (GPC) by Taki Chemical Co., Ltd. (Japan). Solution for the GPC measurement was prepared by dissolving the PLLA sample in tetrahydrofuran (THF). Number-average molecular weight (M_n) and weight-average molecular weight (M_w) were 4.8×10^4 and 9.1×10^4, respectively. These values were calibrated by polystyrene standards. Optical rotatory power, $[\alpha]_D^{25}$, of the sample, which was also measured by them at a wavelength of 589 nm using 0.1% chloroform solution at 25 °C, was −156. The pellets were heated and kept in a vacuum oven at 120 °C for 24 h for the removal of any residual moisture before they were measured.

2.2. Apparatus

A thermal analysis and sample preparation for the X-ray measurements were carried out with a differential scanning calorimeter (Perkin–Elmer Pyris 1). The temperature of the DSC apparatus was calibrated with indium. The heat of fusion was also calibrated with indium. A PLLA sample of about 5 ± 0.1 mg was sealed in an aluminum sample pan for DSC. Samples were used for DSC and were always kept under a nitrogen atmosphere.

All microscopic observations were made with a polarizing microscope (Nikon Eclipse E600-POL, Japan) between crossed polars. The temperature control of a sample was performed using a hot stage (Linkam TH-600PM, Linkam Scientific Instruments, UK). The temperature of the apparatus was calibrated with tin, indium, potassium nitrate, biphenyl, and water at a HR of 0.1 K min^{-1}. Liquid nitrogen was used for the rapid cooling. PLLA resin sandwiched between microscope glass slides was heated to 220 °C on a hot plate and was pressed with small stress to prepare thin film samples with desired thickness. The morphology of the thin film samples between the glass slides was observed on a hot stage and recorded on a hard disk.

Wide-angle X-ray diffraction (WAXD) patterns were obtained at room temperature (ca. 20 °C) with a WAXD measurement system reported elsewhere [23]. Monochromatized Cu K_α radiation (=1.542 Å) was used as an incident X-ray beam. The diffracted X-ray intensity was detected with a position-sensitive proportional counter (PSPC) system. The diffraction angles reported for α-aluminum oxide (α-Al_2O_3) were used as a standard: the angles of the diffraction patterns were corrected with three diffraction angles of α-Al_2O_3 for the Cu K_α radiation: 25.296, 35.152, and 37.801°, corresponding to the reflection lines of (012), (104), and (110), respectively [24].

2.3. Heating and cooling conditions

Vasanthakumari and Pennings [4], Tsuji and Ikada [11], and Kalb and Pennings [15], reported equilibrium melting temperatures (T_m°'s) for PLLA at 207, 205, and 215 °C, respectively. In our experiment, samples were held in a molten state (210 °C) for 10 min for the removal of any crystal nuclei in the samples. The melted samples were cooled to a predetermined crystallization temperature (T_c) at a rate of 70 K min^{-1}, and the isothermal crystallization was performed. At various T_c's ranging from 80 to 140 °C, crystallization isotherms were obtained with DSC, and the growth of spherulites was observed with a polarizing microscope. Hereafter, isothermally crystallized sample obtained at T_c is abbreviated as ICS(T_c). To prevent additional crystallization during cooling from T_c to 30 °C, the ICS was cooled rapidly at a rate of 70 K min^{-1}. The ICSs of 4.0 mm in diameter and 1.0 mm in thickness were prepared for the X-ray measurements.

3. Results

3.1. Peak crystallization time

Fig. 1 shows crystallization isotherms at the indicated T_c's. The scale of the heat flow rate of every crystallization isotherm is normalized, so that their peak heights can be compared with each other. DSC curves are not presented in a temperature range higher than 140 °C and lower than 80 °C, because the exothermic heat flow in a crystallization process is too small to detect by a present thermal analyzer.

Crystallization half-time ($t_{1/2}$), which is defined as a time spent from the onset of the crystallization to the point where the crystallization is 50% completed, has been normally used in the analysis of crystallization kinetics and is taken as a measure of the overall rate of crystallization [25]. It is easily deduced that the completion of the crystallization, i.e.,

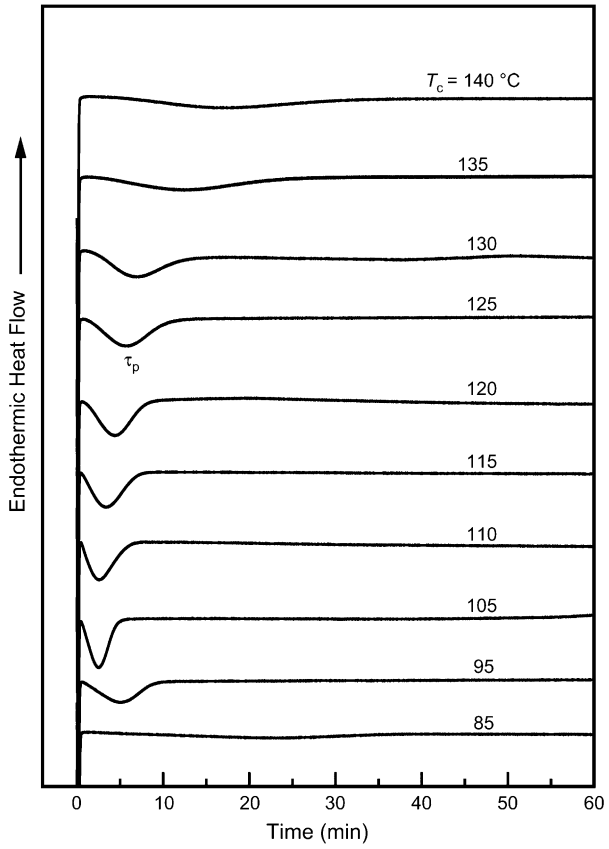

Fig. 1. Crystallization isotherms of PLLA samples at various T_c's. The T_c's are indicated in the figure.

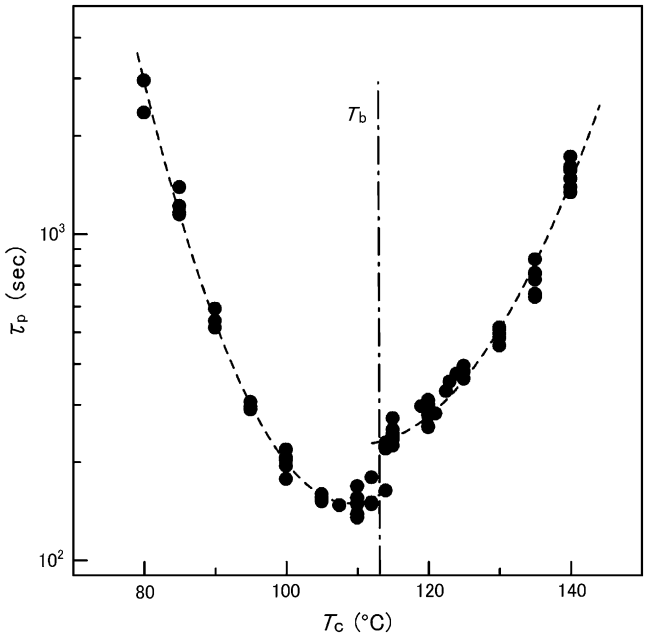

Fig. 2. T_c dependence of the peak crystallization time (τ_p).

final value of the crystallinity, is not easy to determine in semi-crystalline polymers. That is, the crystallization half-time is not easy to accurately determine. To avoid this problem, peak crystallization time (τ_p) is defined as the time spent from the onset to the point where the exothermic peak appears in the crystallization isotherm. Since τ_p is determined from the exothermic heat flow of a whole sample, τ_p can be considered to express the overall rate of crystallization like the crystallization half-time. If peak profile of the crystallization isotherm is symmetric, then the peak crystallization time is the same as the crystallization half-time, i.e., $\tau_p = t_{1/2}$.

Fig. 2 shows the T_c dependence of the peak crystallization time (τ_p) obtained from the crystallization isotherm. The vertical axis is expressed by a logarithmic scale. As can be seen in the figure, τ_p exponentially increases with increasing T_c from 113 °C or with decreasing T_c from about 110 °C, and T_c dependence of $\log(\tau_p)$ discretely changes at 113 °C. The discrete change of τ_p indicates that the crystallization behavior is distinctly different between the low- and the high-temperature ranges, and that change of the crystallization behavior is sensitive to T_c. Hereafter, the boundary temperature between the low- and high-temperature ranges is denoted as T_b and is shown by a dash-dotted line in the figure. As mentioned in the subsequent section, T_b was also determined as 113 °C by the measurement of a linear growth rate of spherulite.

T_c dependence of $\log(\tau_p)$ was fitted by quadratic equations in both temperature ranges, and the fitting curves are shown by the dashed lines. Although the bowl-shaped curves have been reported for the T_c dependence of $\log(t_{1/2})$ for usual crystalline polymers [25], the T_c dependence of $\log(\tau_p)$ shown in the figure is obviously different from them. Characteristics as to the T_c dependence of $\log(\tau_p)$ is as follows. (1) $\log(\tau_p)$ in the T_c dependence of $\log(\tau_p)$ discretely changes at T_b (=113 °C) where is close to the minimum point of $\log(\tau_p)$. That is, there are two temperature ranges in T_c: a high-temperature range ($T_b < T_c$) and a low-temperature range ($T_c < T_b$). (2) The high-temperature curve shifted to upper direction of τ_p against the low-temperature curve. The crystallization rate close to T_b in the high-temperature range ($T_b < T_c$) is distinctly slower than that of the low-temperature range ($T_c < T_b$). (3) The curve of T_c dependence of $\log(\tau_p)$ in the low-temperature range ($T_c < T_b$) is obviously steeper than that in the high-temperature range ($T_b < T_c$).

Crystallization isotherm presented in Fig. 1 shows heat flow during the isothermal crystallization. Heats of crystallization from the start of crystallization to a time of an end of the crystallization and to the peak crystallization time ($0 \sim \tau_p$) were obtained from crystallization isotherms and are denoted by Q_e and Q_p, respectively. That is, Q_e and Q_p were obtained from the heat flow during the isothermal crystallization. Fig. 3 shows T_c dependence of Q_e and Q_p in the temperature range between $T_c = 80$ and 140 °C. The crystallization times were 1 h for $T_c = 95-125$ °C, 2 h for 85, 90, 130, and 135 °C, 3 h for 140 °C, and 7 h for 80 °C. It was elucidated that the peak crystallization time, τ_p, exponentially changes with T_c as shown in Fig. 2. That is, the crystallization time for obtaining the ICSs changes with T_c. The ICS used in this and X-ray experiments was prepared by the crystallization time of approximately four times of τ_p at each T_c.

The baseline for the crystallization isotherm could not be accurately determined. Actually, each value of Q_e for T_c

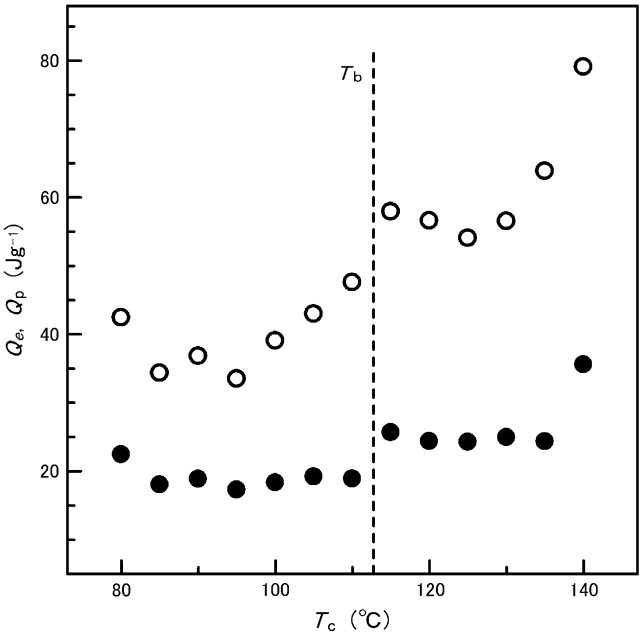

Fig. 3. T_c dependence of Q_e (open circle) and Q_p (filled circle). The crystallization times were 1 h for $T_c = 95$–125 °C, 2 h for 85, 90, 130, and 135 °C, 3 h for 140 °C, and 7 h for 80 °C.

differed from the value of the heat of fusion, which was obtained from the DSC melting curve for the same ICS(T_c) used in this experiment. However, each value for Q_e or Q_p can be compared with each other, because it was obtained by the same procedure. As shown in Fig. 3, T_c dependence of Q_e and Q_p discretely changes at T_b. This discrete change corresponds well with that of τ_p shown in Fig. 2. On the other hand, Q_p does not largely change with T_c.

As shown in Fig. 3, the values for Q_e and Q_p at 140 °C are distinctly different from others. This temperature is high, so that the baseline of the crystallization isotherm deflects as a result of the heat of the additional crystallization due to the annealing effect. It can be considered that Q_e and Q_p were overestimated by the deflection of the baseline at this temperature.

3.2. Morphology

Morphology of the present PLLA samples during isothermal crystallization was studied in a temperature range between 81 and 161 °C under the polarizing microscope: the growth of spherulites was observed between crossed polars at T_c. Fig. 4 shows optical micrographs for the final morphologies at every T_c's. The optical micrographs (a–c) and (d–f) show the morphologies in the low-temperature ($T_c = 81$, 91, 111 °C: $T_c < T_b$) and high-temperature ($T_c = 116$, 121, 126 °C: $T_b < T_c$) ranges, respectively.

In the isothermal crystallization process at $T_c = 81$ °C, a lot of spherulites uniformly appeared in a whole view field of a microscope. These spherulites grew with a slow growth rate. The final morphology of this sample showed granular appearance as observed in (a). In contrast, spherulites did not uniformly appear in the temperature range of T_c between 86 and 111 °C. Then, sparsely distributed spherulites grew. The dimension of the spherulites at the final stage of the crystallization is irregular as observed in (b) and (c). When T_c increased from 111 °C ($T_c < T_b$) to 116 °C ($T_b < T_c$), the final dimension of the resulting spherulites and the uniformity of the dimension evidently increased as observed in (c) and (d). These increases may correspond to the discrete change of the peak crystallization time. With increasing T_c in the temperature range above T_b, the number of spherulite in the view field largely decreased. Consequently, the final dimension of spherulites drastically changed from 121 to 126 °C as shown in (e) and (f).

The optical micrographs (a–d) in Fig. 5 show the morphologies for the samples isothermally crystallized at 126, 131, 141, and 151 °C, respectively. The size of the spherulites considerably increased with increasing T_c. Fig. 5(a) is the same micrograph of Fig. 4(f) on reduced scale. The spherulites evidently showed negative birefringence as reported by many authors [4]. As mentioned in the previous paragraph, number of spherulites in the view field and the growth rate of spherulites drastically decreased with increasing T_c. Roughly speaking, T_c dependence of the morphology corresponds to that reported in literatures [4,10–12].

Periodic extinction band (banded structure), that is, circular ring morphology in the spherulite, is clearly observed in Figs. 4(e) and 5(b). Then, Xu et al. reported that the banded spherulites were observed via the direct isothermal crystallization procedure, and that the banding morphology changed with the melting condition [9]. Although there is an enough possibility to observe the banded spherulites in the ICS obtained in other T_c's, we did not perform further investigation on the formation of the banded spherulites.

3.3. Number of spherulite

As mentioned above, morphology during isothermal crystallization was studied with polarizing microscope. Number of spherulite (N) in the view field was counted at each crystallization temperature in the range from 96 to 141 °C. Sample thickness for the observation was about 2 μm. Fig. 6 shows the crystallization temperature, T_c, dependence of the number of spherulite N observed with a high magnification (×500). A dashed line in the figure shows a fitting curve. When T_c is above 136 °C, the spherulite could be scarcely found in the view field of the high magnification. Accordingly, the number of spherulite was counted with a low magnification (×100) above 136 °C. Then N above 136 °C was obtained by the conversion from the number of spherulite of the low magnification into that of the high magnification.

Since the sample thickness could not be precisely controlled, the accuracy of plotted data is considered not to be high. When T_c is lower than 106 °C, number of the spherulite was too many to accurately count it in spite of the use of picture recorded on a hard disk. That is, there are two problems on the accuracy of the experiment: controlling of the sample thickness and counting of the number of spherulites. However, as shown in Fig. 6, deviation of the plotted data from the fitting curve is small, except for the large change of the plotted data

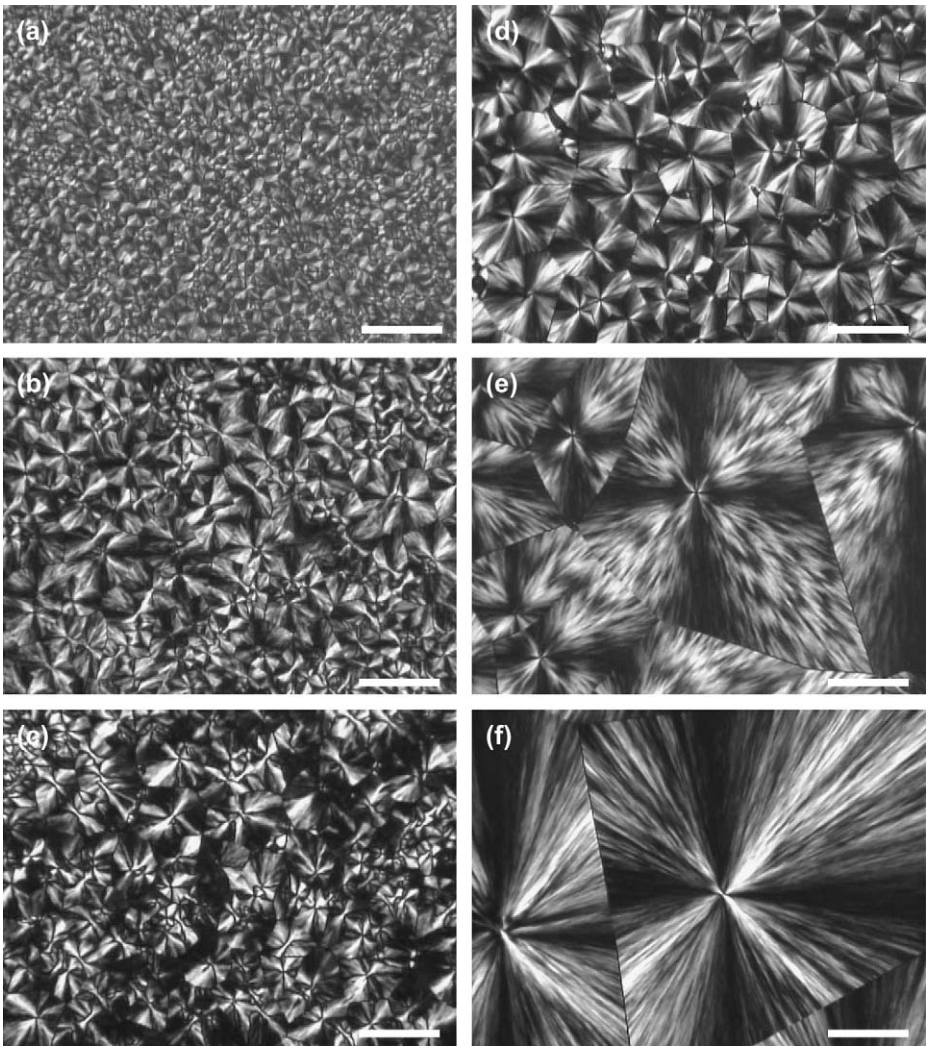

Fig. 4. Optical micrographs between crossed polars for samples isothermally crystallized at (a) 81 °C, (b) 91 °C, (c) 111 °C, (d) 116 °C, (e) 121 °C, and (f) 126 °C. Scale bar shows 50 μm.

at about 122 °C. Since $\log(N)$ almost linearly decreases with T_c in the temperature range above 105 °C as can be seen in the figure, it can be considered that the number of spherulite N exponentially decreases with T_c in this temperature range.

3.4. Radius growth rate of spherulite

The growth process of the spherulite during isothermal crystallization was observed by a polarizing microscope. Then, radius of the spherulite (r) was measured with crystallization time (t), which is defined as the time spent from the onset of the isothermal crystallization of the hot stage. The radius increased linearly with the crystallization time at all T_c's, then radius growth rates G ($G = dr/dt$) were determined at each T_c ranging from 81 to 151 °C. Fig. 7 shows T_c dependence of the radius growth rate G. The vertical axes of (a) and (b) in Fig. 7 are expressed by decimal and logarithmic scales, respectively. The dashed lines show fitting curves for the T_c dependence of G. As shown in Fig. 7(a) and (b), the T_c dependence of G discretely changes at 113 °C. An experimental value for G at 113 °C almost agreed with an average of the two values extrapolated from the fitting curves. Accordingly, the boundary temperature, T_b, was determined as 113 °C and is shown by dash-dotted lines in the figure. This result is well agreed with that determined from the T_c dependence of the peak crystallization time (τ_p).

A bell-shaped curve for the T_c dependence of G is a typical profile of the crystalline polymers as reported by many authors [26–29]. Besides, Umemoto and Okui proposed the master curve which represents the T_c dependence of G for the common polymers including PLLA [30]. On the contrary, the T_c dependence of G presented in this experiment can be divided into two ranges, high- and low-temperature ranges, and is obviously different from the common polymers as shown in Fig. 7. Takayanagi and Yamashita reported discrete change of T_c dependence of G for poly(ethylene adipate) in the low- and high-temperature ranges [31]. This feature on the T_c dependence of G is similar to that obtained in this experiment, except that G in the low-temperature range is smaller than that in the high-temperature range. Additionally, they showed the change of the crystal structure in these two ranges. T_c dependence of G composed of the two bell-shaped curves is similar to that

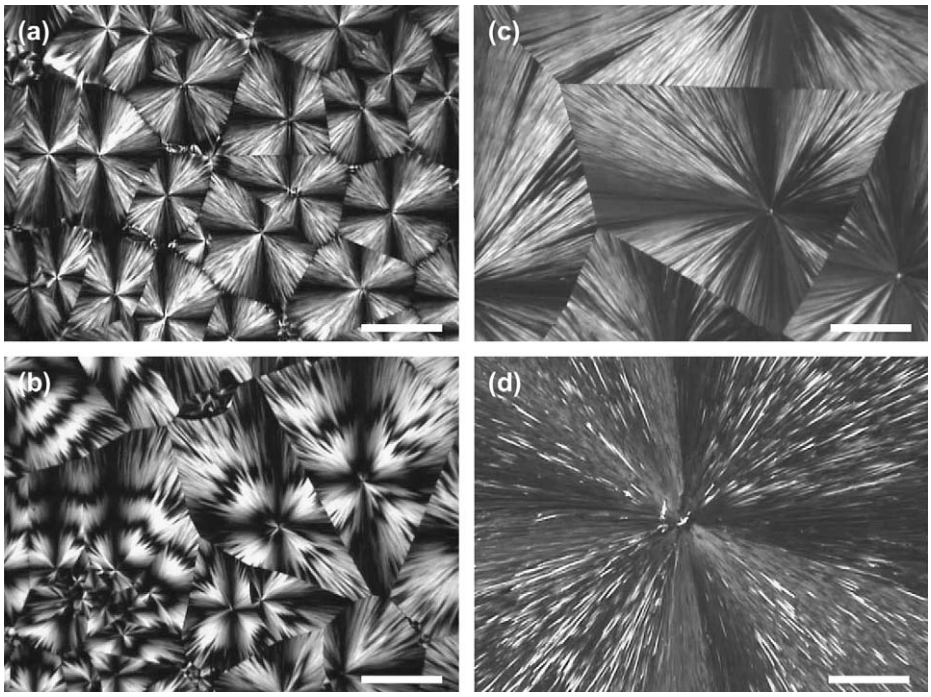

Fig. 5. Optical micrographs between crossed polars for samples isothermally crystallized at (a) 126 °C, (b) 131 °C, (c) 141 °C, and (d) 151 °C. Scale bar shows 250 μm.

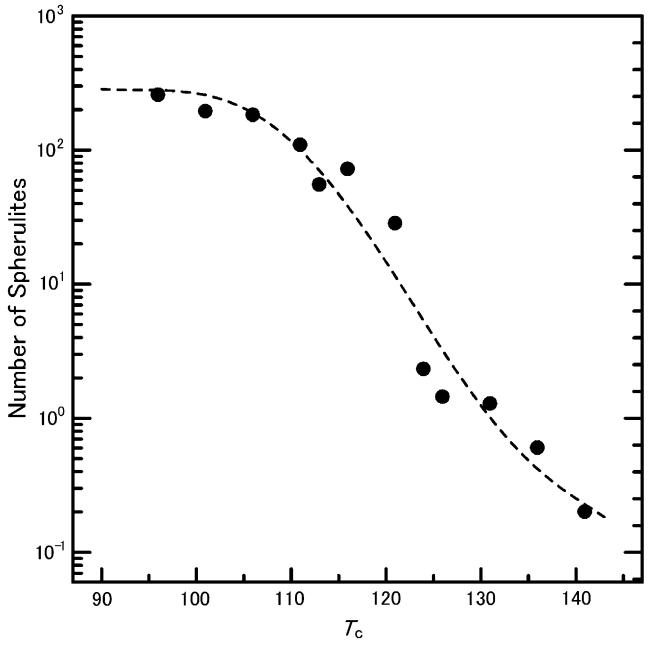

Fig. 6. T_c dependence of log(N). Dashed line shows a fitting curve.

reported by Tsuji et al. [7,8]. However, the present one is completely different from their one. Their bell-shaped curves are continuously connected: they do not have a well defined break at T_b.

As shown in Fig. 7, T_c dependence of G in the high-temperature range ($T_b < T_c$) shows a bell-shaped curve, which is typical profile of the crystalline polymers as reported by many authors [26–29]. The T_c dependence of G in the low-temperature range ($T_c < T_b$) can be considered to show the left half of a bell-shaped curve and is obviously steeper than that in the high-temperature range. The maximum value of G in the low-temperature range ($T_c < T_b$) is larger than that in the high-temperature range. The G value for T_c close to T_b in the low-temperature range was about one and half times as large as that in the high-temperature range: 8.0, 6.1, and 5.2 μm min^{-1} at 111, 113, and 116 °C, respectively. That is, T_c dependence of G discretely changes at T_b. The results on the T_c dependence of G and τ_p clearly indicate that the crystallization behavior is distinctly different between the low-temperature ($T_c < T_b$) and high-temperature ($T_b < T_c$) ranges, and that two crystallization mechanisms should be considered.

Several authors reported the T_c dependence of G for PLLA samples with different molecular weights [4,5,7,8]. They showed that the G value increases with decreasing of molecular weight. The molecular weight of the PLLA sample used in this experiment was $M_w = 9.1 \times 10^4$. The G values obtained in this experiment approximately agree with those for the sample of $M_w = 5.0 \times 10^4$ presented by Miyata and Masuko [5].

3.5. X-ray analysis of crystal modifications

Fig. 8 shows X-ray diffraction patterns of ICSs. Isothermal crystallization temperatures were indicated in the figure. The crystallization times were 1 h for $T_c = 100$–120 °C, 2 h for 90 and 130 °C, 3 h for 140 °C, 4 h for 80 °C, and 24 h for 150 °C. Since scattering X-ray from the amorphous part overlapped on the diffracted X-ray from the crystalline part, X-ray diffraction patterns were obtained after the subtraction of an X-ray scattering pattern of the molten state of PLLA.

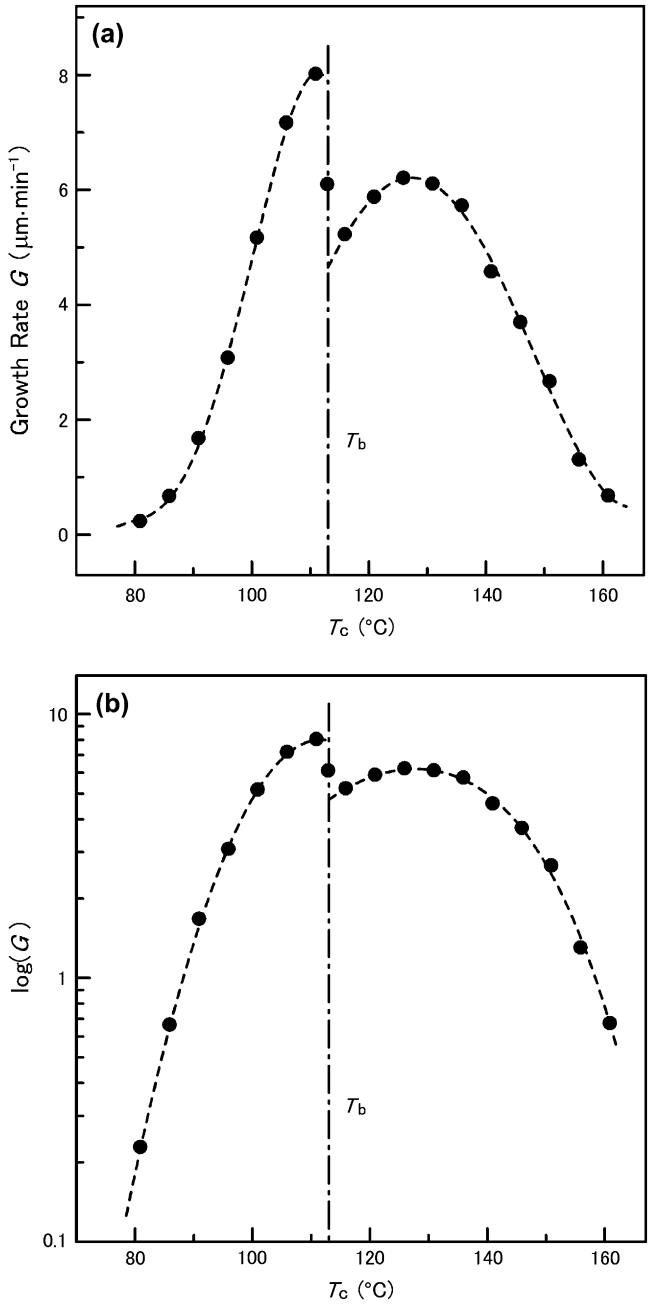

Fig. 7. Crystallization temperature, T_c, dependence of radius growth rate of spherulites, G. (a) G versus T_c and (b) log(G) versus T_c.

The X-ray diffraction patterns in the temperature range $T_c < T_b = 113$ °C are almost same in spite of the small difference in diffraction intensity; similar is for those in the temperature range $T_b < T_c$. In contrast, the X-ray diffraction patterns for the ICSs($T_c < T_b$) are obviously different from those for the ICSs($T_b < T_c$). The diffraction angles of four intense peaks appeared in the diffraction patterns for ICSs($T_b < T_c$) are marked by dotted lines in the figure. The most intense diffraction peak and the next one, appeared at 16.5 and 18.8° for ICSs($T_b < T_c$), shift to lower diffraction angles in the diffraction patterns for ICSs($T_c < T_b$). Small diffraction peaks appeared at 14.7 and 22.5° for ICSs($T_b < T_c$) disappear in the diffraction patterns

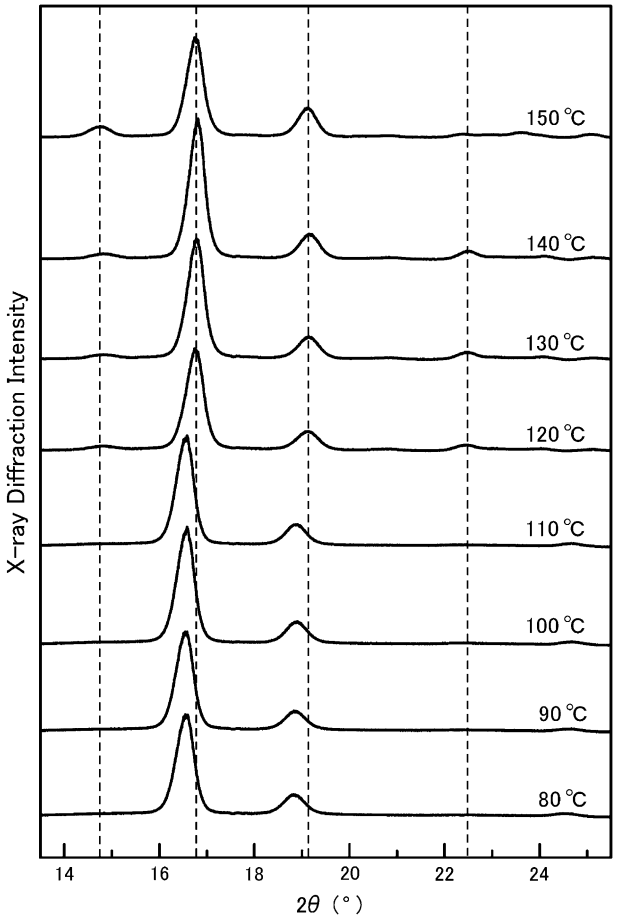

Fig. 8. X-ray diffraction patterns for isothermally crystallized PLLA samples. Crystallization temperatures are shown in the figure.

for ICSs($T_c < T_b$). Accordingly, it can be concluded that the crystal structure of the ICS discretely changes at T_b.

Fig. 9 shows X-ray diffraction patterns between 11 and 36° in 2θ of the ICS(80 °C) and ICS(140 °C). The diffraction pattern for ICS(140 °C) shows many diffraction peaks and agrees well with the orthorhombic crystal structure, which has been assigned as α-form modification [13,14,16]. Cell dimension of an orthorhombic unit cell, $a = 1.06$ nm, $b = 0.60$ nm, $c = 0.94$ nm, may be concluded. The Miller index of five intense diffraction peaks appeared at 12.5, 14.7, 16.7, 19.1, and 22.5° is (101), (010), (110) and (200), (111) and (201), and (102) and (210), respectively. In contrast, the diffraction pattern for ICS(80 °C) shows only four diffraction peaks. This result indicates high symmetry of the crystal lattice. On the other hand, it is difficult from these diffraction peaks to conclusively determine the crystal structure. The diffraction pattern for ICS(80 °C) agreed with the trigonal crystal structure reported as β-form modification. The cell dimension of a trigonal unit cell, $a = 1.07$ nm, $b = 1.07$ nm, $c = 0.99$ nm, may be concluded. The Miller index of the four intense diffraction peaks appeared at 16.5, 18.8, 24.5, and 28.8° is (110), (111), (112), and (300), respectively. The area perpendicular to the c-axis of the unit cell is 0.992 nm^2. Since there are three chains in a trigonal unit cell, the cross-sectional area occupied by a single chain is 0.331 nm^2 which is larger than that of the

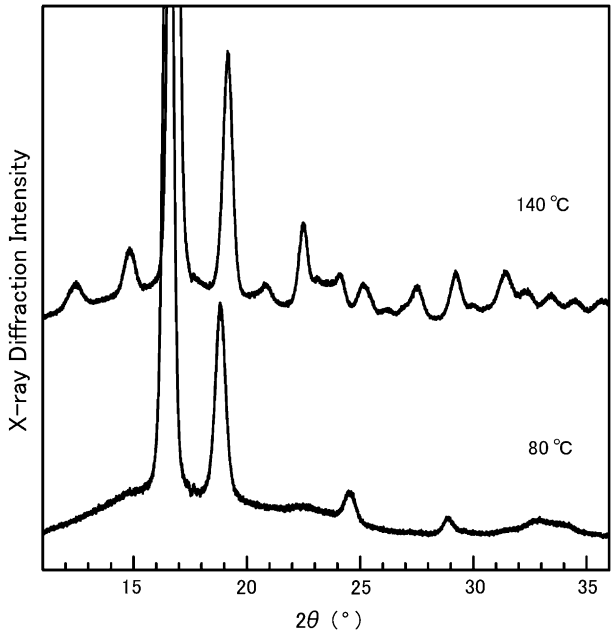

Fig. 9. X-ray diffraction patterns for ICS(80 °C, 2 h) and ICS(140 °C, 24 h).

orthorhombic one (0.321 nm^2) of α-form modification. Consequently, packing of the trigonal modification is interpreted as a *frustrated structure* as suggested by Puiggali et al. [20] and Okihara et al. [22]. It can be presumably concluded from these analyses that the crystal structure of the ICS discretely changes at T_b between orthorhombic crystal modification (α-form) and trigonal one (β-form).

The samples, whose thickness was almost constant, were used for the X-ray measurement, and peak height of the diffraction peaks in Figs. 8 and 9 was not corrected. These are the following characteristics which can be interpreted from these figures. At first, the X-ray diffraction intensity, which can be estimated from the peak heights of the diffraction peaks, increases with increasing T_c, except for the case of the ICS(150 °C). This result indicates the increase of crystallinity of the ICS with increasing T_c. The decrease of the X-ray diffraction intensity for the ICS(150 °C) may mean that the crystallization time of 24 h was not enough for obtaining the ICS which can be compared with the other ICSs. Second, diffraction intensities of the (010) reflection (14.7°) and (111) and (201) reflections (19.1°) in the high-temperature range increase with increasing T_c in comparison with the main peak of (110) and (200) reflections (16.7°). Especially, the increase of the long range ordering of crystal packing can be deduced from the increase of the diffraction intensity of (010) reflection which appears at an angle smaller than that of the main peak of (110) and (200) reflections. The increase of ordering of crystal packing with T_c corresponds to the increase of the regularity of the spherulite morphology with T_c, which is observed by optical microscopy.

The diffraction pattern of ICS(70 °C, 5 h) and ICS(60 °C, 6 h) was also obtained. The diffraction intensity of ICS(70 °C, 5 h) was very small, and that of ICS(60 °C, 6 h) did not appear. These facts indicate that the crystallization scarcely proceeds at a temperature lower than 70 °C.

3.6. Relationship between τ_p and G

As shown in Fig. 2, a trough in a bowl-shaped curve for T_c dependence of τ_p appears below T_b, and there is no trough above T_b. In contrast, a peak in a bell-shaped curve for T_c dependence of G appears above T_b, and there is no peak below T_b as shown in Fig. 7. That is, the trough position of τ_p is different from the peak position of G. Roughly speaking, τ_p is proportional to $1/G$, therefore there is apparent discrepancy between these experimental results. As mentioned in the preceding sections, G represents a growth rate of spherulite, and τ_p corresponds to an overall rate of crystallization. Taking this difference in definition into consideration, following rough estimation is examined to explain the relationship between τ_p and G.

As it is well-known, crystallization proceeds through nucleation and crystal growth, and the number density of a spherulite (nucleus) and growth rate G are significant factors for the crystallization. When there are N spherulites in volume V_0, the number density of the spherulite is N/V_0. For the simplicity of the estimation, it is assumed that N/V_0 does not change during isothermal crystallization, and that the growth of all spherulites starts at the same time. According to this assumption, radius (r) of all spherulites is Gt at time t, and volume of a spherulite is $4\pi r^3/3 = 4\pi(Gt)^3/3$. In addition, the total crystallized volume (V) in the volume V_0 in case of no impingement of spherulites (free growth approximation) would be $4\pi N(Gt)^3/3$. Heat of crystallization from the start of crystallization to t can be obtained from crystallization isotherm and is denoted by Q. Here Q is defined as exothermic heat per unit mass. Accordingly, Q is proportional to V/V_0 and can be written as: $Q = kN(Gt)^3$, where k is proportional coefficient. The heat of crystallization from the start of crystallization to τ_p, that is, Q_p, is

$$Q_p = kN\left(G\tau_p\right)^3. \tag{1}$$

Converting to logarithmic scale, this equation becomes

$$-\log \tau_p = (1/3)\log N + \log G + (1/3)\left(\log k - \log Q_p\right) \tag{2}$$

Fitting curves for $\log N$ versus T_c and $\log G$ versus T_c are shown in Figs. 6 and 7, respectively. The values of Q_p are shown in Fig. 3 and were in the range of 17–36 J g^{-1}. That is, $(1/3)\log Q_p$ is almost constant with T_c in comparison with the change of $(1/3)\log N$ and $\log G$. Therefore, Eq. (2) approximately becomes $-\log \tau_p = (1/3)\log N + \log G + \text{constant}$. According to this approximation, $(1/3)\log N$, $\log G$, and $(1/3)\log N + \log G$ are drawn in Fig. 10.

As shown in the figure, a peak of $(1/3)\log N + \log G$ appears at 107 °C which is below T_b, and there is no peak above T_b. It is easily understood from this figure that T_c dependence curves of $-((1/3)\log N + \log G)$ almost coincide with $\log(\tau_p)$ as shown in Fig. 2 in spite of the small difference of the peak position. The curves for $(1/3)\log N + \log G$ shift along y-axis due to an extra factor $(1/3)(\log Q_p - \log k)$. This coincidence suggests that the two experimental data obtained for $\log(\tau_p)$ and $\log G$ are in accord with each other.

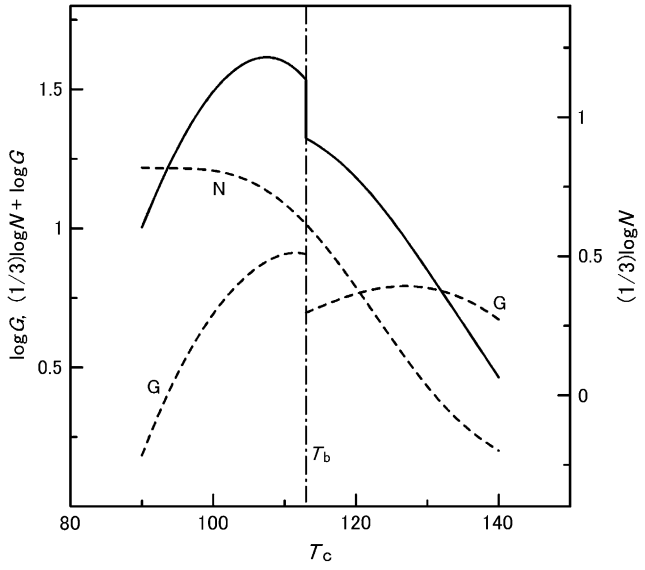

Fig. 10. T_c dependence of $(1/3)\log N$ (dashed line: fitting curve N), $\log G$ (dashed lines: fitting curves G), and $(1/3)\log N + \log G$ (solid lines).

3.7. Crystallization behavior

Crystallization behavior of polymers has been experimentally investigated, and theoretical analysis of the crystallization kinetics has been performed [30–37]. It has been clarified that T_c dependence of G for various polymers, such as nylon 6 [26], poly-(tetramethyl-*p*-silphenylene)-siloxane [27], isotactic polystyrene [28], poly(ethylene terephthalate) [29], shows a bell-shaped curve with a maximum growth rate. This dependence may be described by the following equation [35,37]

$$G = G_0\left[-\frac{\Delta E}{RT_c} - \frac{\Delta F^*}{RT_c}\right] \tag{3}$$

where G_0 is a constant almost independent of temperature, ΔE is the free energy of activation for a chain crossing the barrier to the crystal, and ΔF^* is the free energy of formation of a surface nucleus of critical size.

Vasanthakumari and Pennings [4] and Miyata and Masuko [5] reported a single bell-shaped curve for T_c dependence of G of PLLA, which can be expressed by Eq. (3). On the other hand, Iannace and Nicolais [6] reported that T_c dependence of $10^3/t_{1/2}$ shows two bell-shaped curves, and that a transition from regime II (high temperature) to regime III (low temperature) occurs around 115 °C. However, they did not show the discrete change of $10^3/t_{1/2}$, because number of their data point (10) is too small to determine the curve profile composed of the two bell-shaped curves. Tsuji et al. studied the molecular weight effect on the T_c dependence of G of PLLA and also reported the two bell-shaped curves which are also continuously connected [7,8]. They used small number of data points ($\sim$8) and assigned the two bell-shaped curves to the crystallization of the regime II and regime III. In contrast, it has been presented in this research on the basis of an enough number of data that the crystallization behavior discretely changes at T_b, and that this discrete change originates from the change of the crystal structure. Consequently, the regime analysis was not performed in this study.

Eq. (3) allows T_c dependence of G, which gives a bell-shaped curve, to be explained in terms of two competing processes. Opposing one another are the rate of molecular transport in the melt, which increases with increasing temperature, and the rate of nucleation, which decreases with increasing temperature. Accordingly, diffusion is the controlling factor at lower temperatures, whereas the rate of nucleation dominates at higher temperatures. Between these two extremes the growth rate passes through a maximum where the two factors are approximately equal in magnitude. The bell-shaped curve, which expresses T_c dependence of G, in the high-temperature range $T_b < T_c$ in Fig. 7 can be understood according to this explanation. Besides, the T_c dependence of G in the low-temperature range $T_c < T_b$ is considered as a half of left of the usual bell-shaped curve.

It is shown in this study that G increased 1.6 times by the decrease of T_c across T_b as shown in Fig. 7, and that the molecular chains in the low-temperature range are packed into the disordered, frustrated, crystal lattice (β-form crystal). The formation mechanism of the frustrated crystal has not been proposed yet. Therefore, we examine the following deduction to explain the reason for these results.

Because the crystal structure changes at T_b (trigonal for $T_c < T_b$, orthorhombic for $T_b < T_c$) (1) radial crystallographic orientations, (2) growth planes, and (3) associated energies of chain folding are probably different in the two crystal modifications. The growth rate of the spherulite depends on these factors, so that its discrete change shown in Fig. 7 is deduced to be caused from the difference of these factors in the two crystal modifications. However, further investigation into these factors was not performed in this study.

Since the discrete change of the growth rate originates from the change of the crystal structure, the formation mechanisms of the two crystal modifications are closely connected with the growth rate of the spherulite. Crystallization from the melt has been interpreted to proceed by the process of (i) transport of chain molecules, (ii) their reeling in the crystal surface, (iii) their adhesion on the crystal surface, and (iv) their sliding diffusion on the crystal surface and in the crystal [38,39]. The processes of (i)–(iii) occur in the amorphous phase, therefore they are considered not to discretely change at T_b. On the other hand, the intermolecular distance decreases with decreasing T_c by the decrease of molecular motion. That is, the sliding diffusion of chain molecules on the crystal surface and in the crystal lattice is hindered in the low-temperature range by the decrease of the intermolecular distance. Consequently, there is a possibility that the process (iv) critically changes at T_b by the change of the intermolecular distance. In addition, the helical conformations of the chains in the α- and β-structures have approximately the same energy [14]. Presumably, the chain molecules are packed in the disordered, frustrated, crystal lattice in the low-temperature range by these reasons, and crystal structure discretely changes at T_b.

Although a long time is required for the formation of the ordered crystalline lattice from the melt in which chain molecules are in the disordered state, the time for the formation of the disordered crystalline lattice is shorter than that of the ordered one because of lacking of a long time sliding diffusion process (iv). Consequently, the growth rate of the spherulite G by the decrease of T_c across T_b may be changed by the factor (iv) as well as three factors (1)–(3) mentioned above.

4. Conclusions

Crystallization behavior of PLLA is studied by the thermal analysis, optical microscopy, and X-ray analysis, and following points are elucidated.

1. The curve of the T_c dependence of $\log(\tau_p)$ discretely changes at T_b ($= 113\,^{\circ}C$): its high-temperature region shifted to a long time side of τ_p against its low-temperature region. The crystallization rate close to T_b in the low-temperature range ($T_c < T_b$) is distinctly faster than that in the high-temperature range ($T_b < T_c$).
2. When T_c increased from $111\,^{\circ}C$ ($T_c < T_b$) to $116\,^{\circ}C$ ($T_b < T_c$), the final dimension of the resulting spherulites and the uniformity of the dimension evidently increased. This increase may correspond to the discrete change of the crystallization behavior.
3. The T_c dependence of G discretely changes at T_b ($=113\,^{\circ}C$). The T_c dependence of G and τ_p clearly indicates that the crystallization behavior is distinctly different between the low-temperature ($T_c < T_b$) and high-temperature ($T_c > T_b$) ranges.
4. The X-ray analysis proves that the crystal structure of the ICS discretely changes at T_b. The crystal structures of ICSs($T_b < T_c$) and ICSs($T_c < T_b$) are orthorhombic (α-form) and trigonal (β-form), respectively. The origin of the discrete change in the T_c dependence of τ_p and the T_c dependence of G is attributed to the discrete change of the crystal structure of the ICS at T_b.
5. The relation between the T_c dependence of τ_p and the T_c dependence of G can be explained by the rough estimation in which the number density of spherulites is taken into account.

Acknowledgements

The authors would like to thank Professor Chitoshi Nakafuku (Kochi University, retired) for helpful suggestions and providing us PLLA resin. We are also indebted to Mr. Takao Okada (Medical Material Division, Taki Chemical Co., Ltd.) for measurement of molecular weight and optical rotatory power of PLLA resin.

References

[1] Doi Y, Fukuda K. Biodegradable plastics and polymers. Amsterdam: Elsevier; 1994. p. 577–90.
[2] Smith R, editor. Biodegradable polymers for industrial applications. Cambridge, England: Woodhead Publishing Ltd; 2005.
[3] Tsuji H. In: Doi Y, Steinbuchel A, editors. Polyesters III: applications and commercial products. Biopolymers, vol. 4. Weinheim, Germany: Wiley-VCH; 2002 [chapter 5].
[4] Vasanthakumari R, Pennings AJ. Polymer 1983;24:175.
[5] Miyata T, Masuko T. Polymer 1998;39:5515.
[6] Iannace S, Nicolais L. J Appl Polym Sci 1997;64:911.
[7] Tsuji H, Tezuka Y, Saha SK, Suzuki M, Itsuno S. Polymer 2005;46:4917.
[8] Tsuji H, Miyase T, Tezuka Y, Saha SK. Biomacromolecules 2005;6:244.
[9] Xu J, Guo B-H, Zhou J-J, Li L, Wu J, Kowalczuk M. Polymer 2005;46:9176.
[10] Tsuji H, Ikada Y. Macromolecules 1993;26:6918.
[11] Tsuji H, Ikada Y. Polymer 1995;36:2709.
[12] Tsuji H, Ikada Y. Polymer 1996;37:595.
[13] De Santis P, Kovacs A. Biopolymers 1968;6:299.
[14] Hoogsten W, Postema AR, Pennings AJ, Brinke G, Zugenmaier P. Macromolecules 1990;23:634.
[15] Kalb B, Pennings AJ. Polymer 1980;21:607.
[16] Kobayashi J, Asahi T, Ichiki M, Okikawa A, Suzuki H, Watanabe T, et al. J Appl Phys 1995;77:2957.
[17] Miyata T, Masuko T. Polymer 1997;38:4003.
[18] Aleman C, Lotz B, Puiggali J. Macromolecules 2001;34:4795.
[19] Sasaki S, Asakura T. Macromolecules 2003;36:8385.
[20] Puiggali J, Ikada Y, Tsuji H, Lotz B. Polymer 2000;41:8921.
[21] Catier L, Okihara T, Ikada Y, Tsuji H, Puiggali J, Lotz B. Polymer 2000;41:8909.
[22] Okihara T, Okumura K, Kawaguchi A. J Macromol Sci Phys 2003;B42:875.
[23] Yasuniwa M, Tsubakihara S, Ohoshita K, Tokudome S. J Polym Sci Polym Phys 2001;39:2005.
[24] Berry LG, editor. Powder diffraction file, Inorganic volume PD1S–10iRB. Philadelphia: Joint Committee on Powder Diffraction Standards; 1967. Sets 6–10 (revised).
[25] van Antwerpen F, van Krevelen DW. J Polym Sci A-2 1972;10:2409.
[26] Burnett BB, McDevit WF. J Appl Phys 1957;28:1101.
[27] Magill JH. J Appl Phys 1964;35:3249.
[28] Suzuki T, Kovacs AJ. Polym J 1970;1:82.
[29] van Antwerpen F, van Krevelen DW. J Polym Sci B Polym Phys 1972;10:2423.
[30] Umemoto S, Okui N. Polymer 2002;43:1423.
[31] Takayanagi M, Yamashita T. J Polym Sci 1956;22:552.
[32] Turnbull D. J Appl Phys 1950;21:1022.
[33] Hoffman JD, Weeks JJ. J Chem Phys 1962;37:1723.
[34] Wunderlich B. Macromolecular physics, crystal nucleation, growth, annealing, vol. II. New York: Academic Press; 1976.
[35] Wunderlich B. Macromolecular physics, crystal melting, vol. III. New York: Academic Press; 1980.
[36] Strobl G. The physics of polymers, concepts for understanding their structures and behavior. 2nd ed. Heidelberg: Springer; 1997.
[37] Sperling LH. Introduction to physical polymer science. 3rd ed. New York: John Wiley & Sons; 2001.
[38] Hikosaka M. Polymer 1987;28:1257.
[39] Hikosaka M. Polymer 1990;31:458.